THREE-DIMENSIONAL DENDRITIC SPINE DETECTION BASED ON MINIMAL CROSS-SECTIONAL CURVATURE

Tiancheng He[1], Zhong Xue[1], Yong Kim[2], Stephen T. Wong[1]

[1]Department of Systems Medicine and Bioengineering, The Methodist Hospital Research Institute, Weill Cornell Medical College, Houston, TX; [2] Laboratory of Molecular and Cellular Neuroscience, The Rockefeller University, New York, NY

ABSTRACT

The morphological changes of dendritic spines play a role in adaptive changes of the brain, and dysregulation of them is implicated in various neurological disorders. A systematic analysis tool for the morphology of dendritic spines, acquired via high resolution optical microscopy, should contribute to our understanding of neurophysiology as well as neuropathology. However, large numbers of high-resolution dendritic spine images make manual labeling extremely difficult and laborious. This is particularly challenging for the slender and curved dendritic spines frequently found in the striatum, dysregulation of which is highly implicated in neuropsychiatric diseases, especially when compared to the analysis of relatively small and bulbous dendritic spines in other brain areas, including the hippocampus and cortex, synaptic dysregulation and neurodegeneration, of which are implicated in Alzheimer's disease. In this paper, we present cross-sectional curvature, a new feature, for detecting the tip of dendritic spines in striatal neurons, the spines of which are then segmented using the region growing strategy. Comparative results showed that our method was more accurate and superior to the existing ones.

Index Terms— Dendritic spine labeling, neuron image, segmentation, cross-sectional curvature

1. INTRODUCTION

Dendritic spines are post-synaptic parts of glutamatergic synapses, and regulate synaptic transmission and plasticity. Medium-sized spiny neurons, 95% of all striatal neurons, show highly dense and morphologically versatile dendritic spines[1]. The striatum as a subcortical region of the cerebrum is the major input station of the basal ganglia system. Abnormalities in striatal function are associated with neurological and psychiatric diseases including Parkinsonism, schizophrenia, Attention Deficit Hyperactivity Disorder (ADHD), mental depression and drug addiction. For a better understanding of the physiological and pathological function of striatal neurons, neuroscientists have acquired and analyzed high-resolution images of dendritic spines from pharmacological or genetic animal models of neurological and psychiatric diseases [2-5].

Researchers seek automatic methods in 2D or 3D image processing to analyze dendrites and spines, including classification-based methods and centerline extraction-based methods. Classification-based methods separate points into different groups using a classifier [6]. Centerline extraction-based methods detect all the possible centerlines and treat dendritic spines as small protrusions attached to the dendrites. Various mathematical models have been applied for this method, such as the thinning method proposed by Koh *et al*. [7]. Janoos *et al*. [8] presented a method for dendritic skeleton structure extraction using a curve-skeleton approach based on the medial geodesic function, which is defined on the reconstructed isosurfaces. Recently, more effective methods were presented by Fan *et al*. [9] and Zhang *et al*. [10]. They used a local binary fitting model of level sets and curvilinear structure detectors for spine segmentation.

These previous works and their algorithms were optimized for, or better detectable for, the short types of spines with less variety, but not for the slender and curved spines frequently found in the striatal neurons. To accurately and efficiently detect spines with different shapes, this paper reports that cross-sectional curvature plays a more important role in detecting the tip area of spines than the complicated skeleton or level set methods. We argue that, by performing standard background filtering, the images are quite clear in terms of segmenting the dendritic spines from the background, and therefore a major challenge is performing a shape analysis to detect and segment spines from dendrites. From the complex shapes, we can see that, given various shapes of spines, their commonality is that they have a tip area that distinguishes them from dendrite and spine walls. A distinctive feature of such shapes is that the minimal cross-sectional curvatures on the surface of the dendritic spines will be significantly larger on the spine tip area than on the others.

In this paper, we propose a new feature called minimal cross-sectional curvature for labeling the tips of spines and separating them from the dendrite surface. A traditional region growing method is utilized to segment the spines. Automatic spine labeling can then be achieved.

In experiments, we quantitatively compared the spine detection accuracy with previous methods, and the results showed that our method is accurate and superior.

2. METHOD

We propose a minimal cross-sectional curvature to detect the tip of spines. Then, the whole spine can be segmented by performing region growing.

2.1 Detection of the Spine Tip Area Using Minimal Cross-Sectional Curvature

2.1.1 Cross-Sectional Curvature

Curvature reflects the shape of a curve or a surface and is a common feature for shape analysis. However, when applied to a 3D tubular structure, the curvature along the side wall and the rounded tip are similar, and it is difficult to distinguish the tip from the side wall using 3D curvature. To solve this problem, the cross-sectional curvature can provide more information about the 3D shape. As shown in Fig. 1, given a point P on the surface, a 2D cross-sectional image can be obtained by using a plane T crossing P to "cut" the 3D object. Then, the 2D curvature calculated at point P in the cross-sectional image reflects the shape of the object in plane T. Specifically, the 2D cross-sectional curvature $K(T)$ at point P is defined as the Gaussian curvature.

$$K(T)=\frac{d^2C(p)}{dp^2}\Bigg/\left(1+\left(\frac{dC(p)}{dp}\right)^2\right)^{3/2}, \qquad (1)$$

where C represents the object curve [11-12].

In fact, given a surface point from a dendritic spine image, we can obtain many cross-sectional images as long as the cutting plane T passes through point P. To reflect the 3D object shape at point P, multiple 2D cross-sectional curvatures can represent the detailed shape information better than a 3D curvature.

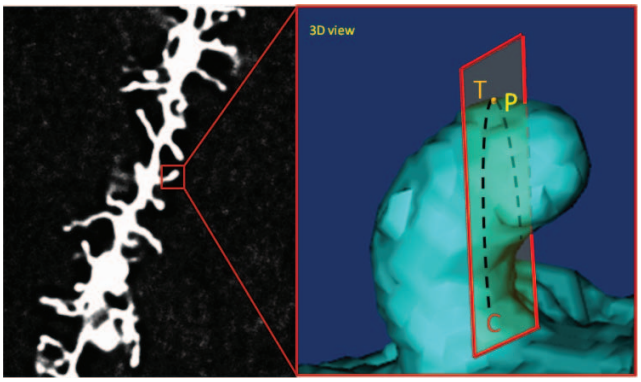


Figure 1. Cross-sectional plane (T) of 3D dendritic spine surface when viewed from a particular angle, the cross-sectional curvature at dendritic spine surface point P is the Gaussian curvature of sectional curve C on plane T.

2.1.2 Detection of the Spine Tip Area Using Minimal Cross-Sectional Curvature

For each surface point P, a cross-sectional curvature $k(T)$ series can be calculated by changing the rotation angle of T. After the cross-sectional curvatures of a point P are calculated, we set the minimal value of them as the feature of point P. The rationale for calculating the minimal cross-sectional curvature is that it can be used to effectively distinguish the tip and side areas of a tubular structure. For points close to the tip area, we can always obtain big cross-sectional curvatures no matter the angle of the cutting plane T, but for the tubular side wall, when the plane is parallel with the tubular structure, small curvature can be obtained. When the plane is perpendicular to the tubular structure, the result is big curvature. To calculate such a minimal cross-sectional curvature, we set the initial cross-sectional plane T_0 to pass through point P and be parallel with the X-Y plane. Then, the plane T_0 is rotated, centering on P, to get other cross-sectional images. Any cross-sectional plane can be achieved after two clockwise rotations on two orthogonal axes. A new cross-sectional plane T after rotation can be denoted as

$$T = M_1 \times M_2 \times T_0 \qquad (2)$$

where M_1 and M_2 are the basic 3D (gimbal-like) rotation matrices around the X and Y axes. We denote the two rotation angles as (α,β) (as shown in Figure 2).

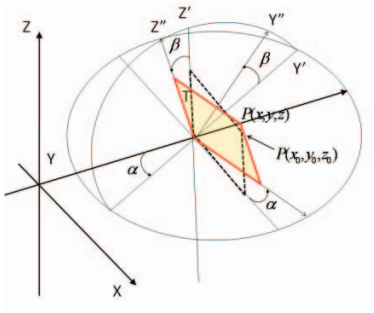


Figure 2. Two rotating transformations in 3D, where (α,β) are two clockwise rotation angles on the X and Y axes.

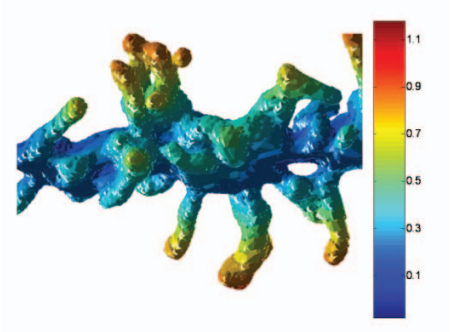


Figure 3. The minimal cross-sectional curvatures are large on spine tips.

After obtaining all the cross-sectional planes T, and calculating the corresponding 2D cross-sectional curvatures according to Eq. (1), we can get the minimal cross-sectional curvature $k(T)$ as,

$$k(T) = \arg\min_{(\alpha,\beta)} \{K(\alpha,\beta)\}. \quad (3)$$

In practice, we rotate the plane by increasing (α,β) 45 degrees each time. Fig. 3 shows the minimal cross-sectional curvatures on the surface of the dendritic spines. It can be noted that the values are larger on the tip area of the spines and smaller otherwise.

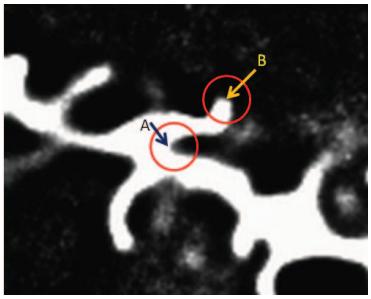


Figure 4. Spine root points are filtered out by calculating the proportion of object points within the spherical area.

Another potential pitfall is that the minimal cross-sectional curvature (absolute value) might be bigger at the root of the spines. As shown in Figure 4, in order to distinguish the regions of A and B, we set a spherical neighborhood for each surface point, and calculate the proportion of the object point versus the total number of points within the sphere. Because more object points are enclosed in the spherical region, we can filter out those points by setting a threshold to the object proportion value (here we set it to 0.5).

2.2 3D Dendritic Spine Segmentation

After detecting the spine tips, we performed traditional region growing on the neuron image. Fig. 5 shows an example of the calculated minimal cross-sectional curvatures. After calculating minimal cross-sectional curvatures, spine tips are detected using thresholding. Then, a region growing method is applied to segment the spines.

3. RESULTS

Fifteen fluorescent neuron images were collected from the research group at the Rockefeller University. These images were taken using a confocal microscope (Zeiss LSM 510) with an oil immersion lens (EC Plan-Neofluar 100×, 1.4 N.A.) and a 2.8x digital zoom. DiI was excited using the Helium/Neon 543 nm laser line. For dendritic spines, a stack of images was acquired in the Z dimension with an optical slice thickness of 0.12 μm. The resolution along X and Y directions is 0.06 μm.

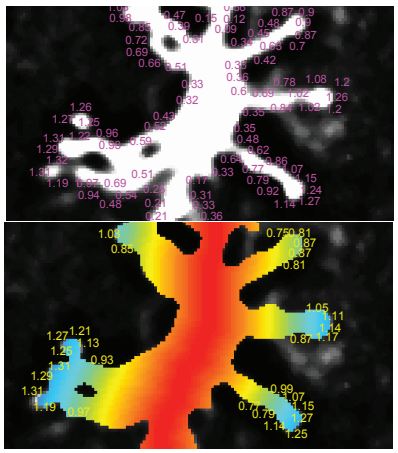


Figure 5. A simple threshold of the calculated minimal cross-sectional curvatures can be applied to detect the spine tips, and region growing can then be applied to segment the spines. Top: example of the minimal cross-sectional values; bottom: region growing from the initial spine tip points after thresholding. Color-map shows the arrival time or the region growing.

To validate the performance of our algorithm, we used the spines manually detected in TMHRI and compared the detection performance of our algorithm with the other three state-of-the-art neuronal spine detection algorithms, as well as the ground truth. The comparison methods are from Rodriguez *et al.*[6], Zhou *et al.*[9], and Zhang *et al.*[10]. As mentioned above, the method from Rodriguez is classification-based using a certain classifier, of which the criteria may cause spurious spines. Zhou and Zhang used a local binary fitting model of level sets and curvilinear structure detection, which may lose 3D information.

Before feature extraction, the regularized Wiener filter is applied to eliminate low-contrast noise, and the Otsu thresholding procedure is employed to separate the neuron points from the background to remove noise. Then, we calculate the cross-sectional curvature on each surface voxel. (α,β) ranges between 0^o and 180^o, and we calculate cross-sectional curvature $K(T)$ by rotating the plane 45^o every time. Notice that, to simplify the calculation, we can first detect the surface points from the preprocessed images, rotate the entire image according to the prescribed angles (α,β), find the corresponding surface points in the new images, and then calculate the 2D curvature of each boundary point in the axial plane. The minimal cross-sectional curvature $k(T)$ of each point is then calculated, and the threshold for detecting spine tips is set as 0.7.

Fig. 6 shows a typical result of our algorithm, including the three cross-sectional views of the original input image and rendering of color-labeled spines. Fig. 7 shows four of our experimental results by 3D rendering of the segmented spines. The quantitative comparison results are shown in Table 1. The range of spine amounts in our neuron images is 50-70. Table 1 shows that our algorithm achieved a higher

accuracy than other detection algorithms. In particular, our algorithm had fewer missing spines and achieved a lower false positive rate. This demonstrates that the minimal cross-sectional curvature can precisely describe the feature of the spine tip. On average, the sensitivity and specificity values are improved by 3% when comparing our method with previous methods.

The software package of this paper was written in Microsoft Visual C++ with graphic user interface (GUI) and is publicly available in our Department's website (www.cbi-tmhs.org).

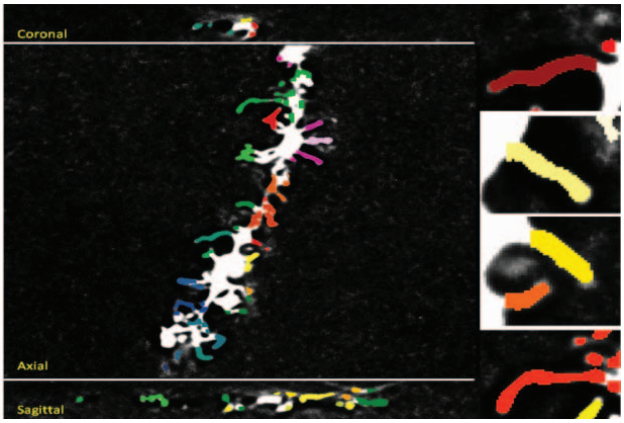


Figure 6. A typical segmentation result of our algorithm, including the three cross-sectional views (Coronal, Axial, Sagittal) of the original input image. Right: the detailed rendering of color-labeled spines.

Our future work will refine the region growing method to precisely cover the spine area in order to classify the spines into different types, and measure their detailed shapes.

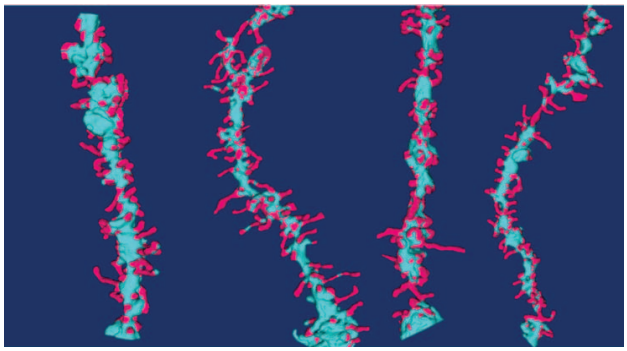


Figure 7. Four of our experimental results by 3D rendering.

Table 1. Comparison of spine detection results using different methods.

Data	Sensitivity	Specificity
Rodriguez	92%	90%
Fan	93%	91%
Zhang	94%	92%
Our method	97%	95%

4. CONCLUSION

We proposed a spine tip detection and segmentation method aiming at speeding up the study of neural morphology in 3D high resolution images. The new minimal cross-sectional curvature is proposed as a distinctive feature for distinguishing spine tips from dendrites in which a region growing method is applied to segment the spines. Quantitative comparison was also performed by comparing the proposed feature-based segmentation with previous algorithms using manual segmentation as the ground truth. The results showed that the proposed algorithm outperformed other methods in terms of sensitivity and specificity for spine detection.

ACKNOWLEDGEMENTS

The authors would like to thank the support of NIH R01 LM009161, R01 AG028928, and TT and WF Chao Center for BRAIN at The Methodist Hospital Research Institute

5. REFERENCES

[1] H. Shen, *et al.*, "Automated quantification of dendritic spine density and spine head diameter in medium spiny neurons of the nucleus accumbens," *Brain Struct Funct,* vol. 213, pp. 149-57, Sep 2008.

[2] D. J. Christoffel, *et al.*, "IkappaB kinase regulates social defeat stress-induced synaptic and behavioral plasticity," *J Neurosci,* vol. 31, pp. 314-21, Jan 5 2011.

[3] Y. Kim, *et al.*, "Phosphorylation of WAVE1 regulates actin polymerization and dendritic spine morphology," *Nature,* vol. 442, pp. 814-7, Aug 17 2006.

[4] Y. Kim, *et al.*, "Methylphenidate-induced dendritic spine formation and DeltaFosB expression in nucleus accumbens," *Proc Natl Acad Sci U S A,* vol. 106, pp. 2915-20, Feb 24 2009.

[5] K. W. Lee, *et al.*, "Cocaine-induced dendritic spine formation in D1 and D2 dopamine receptor-containing medium spiny neurons in nucleus accumbens," *Proc Natl Acad Sci U S A,* vol. 103, pp. 3399-404, Feb 28 2006.

[6] A. Rodriguez, *et al.*, "Automated three-dimensional detection and shape classification of dendritic spines from fluorescence microscopy images," *PLoS One,* vol. 3, p. e1997, 2008.

[7] I. Y. Koh, *et al.*, "An image analysis algorithm for dendritic spines," *Neural Comput,* vol. 14, pp. 1283-310, Jun 2002.

[8] F. Janoos, *et al.*, "Robust 3D reconstruction and identification of dendritic spines from optical microscopy imaging," *Medical Image Analysis,* vol. 13, pp. 167-179, Feb 2009.

[9] J. Fan, *et al.*, "An Automated Pipeline for Dendrite Spine Detection and Tracking of 3D Optical Microscopy Neuron Images of In Vivo Mouse Models," *Neuroinformatics,* vol. 7, pp. 113-130, Jun 2009.

[10] Y. Zhang, *et al.*, "A neurocomputational method for fully automated 3D dendritic spine detection and segmentation of medium-sized spiny neurons," *Neuroimage,* vol. 50, pp. 1472-1484, May 1 2010.

[11] L. P. Eisenhart, "Generalized Riemannian Geometry," *Proc Natl Acad Sci U S A,* vol. 48, pp. 1529-31, Sep 1962.

[12] L. P. Eisenhart, "Generalized Riemannian Geometry, II," *Proc Natl Acad Sci U S A,* vol. 49, pp. 18-9, Jan 1963.